論文 / 著書情報
Article / Book Information

Title	Viscoelasticity and Morphology of an Organic Hybrid of Chlorinated Polyethylene and N,N'-dicyclohexyl-2-benzothiazolyl sulfenamide
Author	Shuichi Akasaka, Toshiki Shimura, Suguru Sasaki, Yoichi Tominaga, SHIGEO ASAI, Masao Sumita
Journal/Book name	Composite Interfaces, Vol. 12, No. 7, pp. 637-653
発行日 / Issue date	2005, 7
URL	http://www.tandfonline.com/loi/tcoi20
Copyright	This is an electronic version of an article published in Composite Interfaces, Vol. 12, No. 7, pp. 637-653.
Note	このファイルは著者（最終）版です。 This file is author (final) version.

Viscoelasticity and morphology of organic hybrid comprising of chlorinated polyethylene and N,N'-dicyclohexyl-2-benzothiazolyl sulfenamide

Shuichi Akasaka, Toshiki Shimura, Suguru Sasaki,

Yoichi Tominaga, Shigeo Asai and Masao Sumita*

Department of Chemistry and Materials Science, Tokyo Institute of Technology,
2-12-1-S8-38, Ookayama, Meguro-ku, Tokyo 152-8550, Japan

*** Corresponding author: Masao Sumita**
Tel:03-5734-2431
Fax:03-5734-2876
E-mail: msumita@o.cc.titech.ac.jp)

Running Head(50char.): viscoelasticity and morphology of organic hybrid

Abstract:

The viscoelasticity and morphology of organic hybrid comprising of chlorinated polyethylene (CPE) and N,N'-dicyclohexyl-2-benzothiazolyl sulfenamide (DBS) were studied by means of tensile and shear complex modulus and differential scanning calorimetry (DSC) analysis. Tensile and shear loss modulus (*E"* and *G"*), which are shown as indexes of vibration damping performance, showed one peak corresponding to the glass transition. The peak maximum values ($E"_{max}$ and $G"_{max}$) increased in proportion to DBS content (ϕ_{DBS}) and the slope of $E"_{max}$ against ϕ_{DBS} became steep above a certain DBS content, i.e. the critical DBS content (ϕ_c). A high damping material was obtained by the addition of DBS, especially when DBS content was higher than ϕ_c. These increases in loss moduli below and above ϕ_c are caused by the interaction between CPE and DBS molecules and the friction between DBS molecules, respectively. It was found that CPE/DBS is a compatible blend at all DBS contents from the analysis of the glass transition temperature with DSC. Furthermore, the influence of chlorine content in CPE on those characteristics was investigated. Higher chlorine content led to lower ϕ_c, a decrease in *E"* below ϕ_c and an increase in *E"* above ϕ_c, These results are due to the increase in the number of dichloromethylene units (CCl_2), which reduces the α-hydrogen atom in CPE.

Keyword:

Chlorinated polyethylene (CPE), N,N’-dicyclohexyl-2-benzothiazolyl sulfenamide (DBS), organic hybrid, viscoelasticity, morphology, compatibility, vibration damping, glass transition

1. Introduction

There are many investigations on damping materials, because vibrations are undesirable for the living environment and electrical and mechanical fields requiring precise control. When a material is vibrated by external mechanical energy, vibration energy is converted into heat energy by molecular friction. And then, dissipation of heat energy results in vibration damping. On the basis of friction theory, the magnitude of friction is determined by the following three factors; normal force, coefficient of friction and sliding distance [1]. Considering the friction in vibrating material, we supposed that those three factors correspond to molecular packing, the number and the strength of interaction between molecules, and relative displacement of molecules by external energy, respectively. Till now, damping performance of polymer has been improved by polymer blending, copolymerization, the addition of inorganic filler and so on. We focused on the organic low molecular weight compound in an amorphous state. The low molecular weight compound showing strong interaction or having complicated structure forms an amorphous phase by quenching from the melt. Such compound shows tighter packing and forms interactions more readily than the amorphous polymer, since adjacent segments limit the arrangement and movement of segments in the polymer. Moreover, relative displacement by external energy is greater than that of the polymer, in which entanglement of molecular chain and the limitation of segmental motion by

adjacent segments are present. So, it is supposed that such a compound is a better damping material than an amorphous polymer. However, the pure organic low molecular weight compound in an amorphous state is too soft to maintain the shape above the glass transition temperature. Therefore, the viscoelasticity of the organic hybrid materials comprising of low molecular weight organic compound and a polymer was studied in anticipation of high damping performance by the low molecular weight organic compounds while the polymer retains specimen shape.

Viscoelasticity of organic hybrid materials comprising of rubbery amorphous polymers [2-7] such as chlorinated polyethylene (CPE) or acrylic rubber, and vitrified low molecular weight organic compounds such as N,N'-dicyclohexyl-2-benzothiazolyl sulfenamide (DBS) or 4,4'-Thio-Bis(3-methyl-6-tert-buthylphenol) (BPSR) or 3,9-bis{1,1-dimethyl-2[b-(3-tert-butyl-4-hydroxy-5-methylphenyl)propionyloxy]ethyl}-2,4,8,10-tetraoxaspiro[5,5]-undecane (AO-80). The viscoelasticity and morphology of CPE/DBS had been reported by Inoue et al. [2] and Wu et al. [3]. They found that the peak maximum value of loss modulus (E''_{max}) and loss tangent area (TA) increased in proportion to DBS content (ϕ_{DBS}) at lower ϕ_{DBS}, where TA is defined as the peak area around the glass transition in the temperature dependence of loss tangent ($\tan\delta$). And, the slope of those values against ϕ_{DBS} became steep above certain DBS content, referred as the critical DBS content (ϕ_c). Inoue et al. reported that the phase state was

semi-compatible below ϕ_c, and compatible above ϕ_c for CPE (Chlorination degree: 30wt%)/DBS. On the other hand, Wu et al. considered that the rapid increase in TA above ϕ_c for CPE (Chlorination degree: 40wt%)/DBS came from the occurrence of phase separation and crystallization of DBS molecules.

In this study, we report on the viscoelasticity and morphology of organic hybrid materials comprising of CPE and DBS, since we obtained different considerations with previous papers mentioned above. In addition, we investigated the influence of chlorine content in CPE on these characteristics.

2. Experimental

CPEs with chlorine content of 32 wt% and 40 wt% (Elaslene 301A and 401A, Showa Denko K.K., JAPAN) were used as matrix polymer. The CPEs are designated as CPE32 and CPE40, respectively. Table 1 shows the molecular weight determined with gel-permeation chromatography (GPC). The DBS (shown as Figure 1, Nocceler DZ, Ouchishinko chemical industrial Co., Ltd., JAPAN) was used as an organic low molecular weight compound. DBS is normally used as an accelerator in sulfur vulcanization, but it is not effective below 190 ^{o}C without sulfur. The material was kneaded with a two-roll mill at 60 ^{o}C. Then, the mixture was melt-pressed at 140 ^{o}C for 10 min under the pressure of 19.6 MPa followed by quenching in iced-water to obtain an amorphous film with a thickness of about 1 mm. All measurements were conducted within a few hours after compression to measure in the amorphous state.

Dynamic mechanical analysis (DMA) was carried out with IT-DVA200s (ITK Co., Ltd., JAPAN) in the oscillatory tensile mode. Then we obtained the temperature dependence of tensile storage modulus (*E'*), tensile loss modulus (*E"*) and tensile loss tangent ($\tan\delta_E$). The oscillation strain was 0.1 % at a frequency of 10 Hz and a heating rate was 5 ^{o}C/min. The sample dimensions were 5 mm in width and 1 mm in thickness and the distance between clamps is fixed 20 mm.

The temperature dependence of shear storage modulus (*G'*), shear loss modulus (*G"*) and shear loss tangent ($\tan\delta_G$) were measured with PHYSICA UDS200 (Anton Paar Co. Ltd., Germany) using a parallel plate of 8 mm in the oscillatory shear mode. The shear strain was 0.01 % at a frequency of 10 Hz and the normal force was fixed 5 N. The heating rate was 5 ^{o}C/min.

Differential scanning calorimetry (DSC) curves were obtained with DSC8230 (RIGAKU Co., JAPAN) at the heating rate of 5 ^{o}C /min under nitrogen atmosphere. The sample weight was about 5 mg.

3. Results and Discussion

Initially, the viscoelasticity and morphology of CPE32/DBS was discussed. Figure 2 shows the temperature dependence of *E'*, *E"* and $\tan\delta_E$ of CPE32/DBS with different ϕ_{DBS}. Only one glass transition was observed. As ϕ_{DBS} increased, the glass transition temperature (T_g), obtained from the middle point of the glass transition in *E'* and the peak temperature of *E"* and $\tan\delta_E$, shifted to higher temperature. And the temperature width of the glass transition in *E'* and the peak width of *E"* and $\tan\delta_E$ became narrower with increasing ϕ_{DBS}. Generally, the relationship between compatibility and the glass transition behavior is well known as follows [8]: In the case of highly compatible blends, the single T_g of the blend shifts gradually between the T_gs of each pure component while the glass transition width of the blend does not broaden beyond those of pure components. As compatibility decreases, the glass transition width of the blend becomes broader than that of pure components. Then, in the case of incompatible blends, the two glass transitions corresponding to two phase-separated domains appear. If the two T_gs of phase-separated domain are close, the glass transition of incompatible blends is shown as one transition, but the glass transition width becomes broader than that of pure components by superposition of two peaks. It was, therefore, found CPE32/DBS was a compatible blend, since only one glass transition was observed and its temperature width did not broaden. The suppression of softening

by CPE was evaluated by the value of E' at 50 ^{o}C, which is the temperature above T_gs for all samples. That value decreased with increasing ϕ_{DBS}. The tensile modulus of pure DBS could not be measured, since is too soft to apply the sufficient oscillating strain and static stress for DMA measurement. That is to say, the polymer chain of CPE prevented the softening by DBS. The values of E'' and $\tan\delta_E$ are well known as the indexes of vibration damping performance. It was found that vibration damping performance was improved by the addition of DBS molecules, because the peak maximum value of E'' (E''_{max}) and $\tan\delta_E$ ($\tan\delta_{Emax}$) increased with ϕ_{DBS}.

To investigate the influence of ϕ_{DBS} on vibration damping performance, Figure 3 (a) and (b) shows the dependence of E''_{max} and $\tan\delta_{Emax}$ on ϕ_{DBS}, respectively. The value of $\tan\delta_{Emax}$ increased nonlinearly with ϕ_{DBS}. Figure 4 shows the dependence of E' and E'' at the peak temperature of $\tan\delta_E$ on ϕ_{DBS}, because $\tan\delta$ is defined as the ratio of E'' to E'. The value of $\tan\delta_{Emax}$ is also shown as a reference in Figure 4. Both E' and E'' decreased with increasing ϕ_{DBS}. In particular, E' showed a greater decrease than E'', resulting in an increase in $\tan\delta_{Emax}$. In other words, the increase in $\tan\delta_{Emax}$ is caused by not the increase in E'', corresponding to energy loss, but the decrease in E'. For this reason, E''_{max} is more suitable than $\tan\delta_{Emax}$ for investigation on damping behavior. The value of E''_{max} increased in proportion to ϕ_{DBS}. And the slope of E''_{max} against ϕ_{DBS} became steep above DBS content of about 49 wt%. The ϕ_{DBS} at the bending point of the

slope is designated as the critical DBS content (ϕ_c). Below ϕ_c, DBS molecules dispersed homogeneously in the CPE matrix while DBS molecules interacted with CPE chains, because CPE32/DBS is a compatible blend. It was reported CPE showed compatibility with poly(methyl methacrylate) (PMMA) [9-11], ethylene-vinyl acetate copolymer (EVA) [12] and polycaprolactone (PCL) [13] by forming hydrogen bonding between the α-hydrogen atom in CPE and the carbonyl functional groups in those polymers. It was, therefore, considered that the α-hydrogen atom in CPE interacted with a benzothiazolyl functional group in the DBS molecule, including the π-electron in benzene ring and an unpaired electron of a nitrogen atom. The value of E''_{max} below ϕ_c was increased by this interaction, which formed in proportion to the amount of DBS molecules. On the other hand, to investigate the damping behavior above ϕ_c, we needed to measure viscoelasticity of pure DBS. However, we could not measure tensile complex modulus of pure vitrified DBS as mentioned above. For that reason, we carried out the shear complex modulus measurement, which is measurable even for pure DBS.

The temperature dependence of shear complex modulus (G', G'' and $\tan\delta_G$) shows similar tendency with that of tensile complex modulus as shown in Figure 2. Figure 5 shows the dependence of the peak maximum value of G'' (G''_{max}) on ϕ_{DBS}, respectively. The values of G''_{max} for pure DBS and CPE32/DBS above ϕ_c lay on a straight line. The main cause of an energy loss of pure DBS is the friction between DBS

molecules. Consequently, the rapid increase in E''_{max} and G''_{max} above ϕ_c is caused by the friction between free DBS molecules, forming no interaction with CPE.

Figure 6 shows the DSC curves of CPE32/DBS blend. Although a slight melting peak of CPE around 105 ^{o}C for the samples with lower DBS content was observed, pure CPE was amorphous polymer since the peak area is too small. The samples with ϕ_{DBS} above 50 wt% showed the crystallization and melting peaks of DBS. Since each of the two peaks had almost equal area, it was confirmed DBS in quenched CPE/DBS formed amorphous phase. The crystallization of DBS during heating process is caused by free DBS molecules, which easily aggregate. Figure 7 shows the dependence of the onset, the middle point and the endset temperatures of glass transition obtained from Figure 6 on ϕ_{DBS}. The middle point temperature of glass transition was defined as the T_g in DSC measurement. The width of glass transition, which is the difference between onset and endset temperatures, was unchanged or slightly reduced. The T_g shifts to higher temperature nonlinearly with increasing ϕ_{DBS}. The relationship between T_g and the composition of the blend expresses by Gordon-Taylor equation [14] written as follows:

$$T_g = \frac{w_1 \cdot T_{g1} + K \cdot w_2 \cdot T_{g2}}{w_1 + K \cdot w_2} \quad (1)$$

where T_g is the glass transition temperature of the blend and w_i and T_{gi} are the weight

fractions and glass transition temperature of the *i*-th component and *K* is an adjusting parameter, expressing the degree of curvature in the T_g-composition diagram. Moreover, *K* gives semi-empirically the index of the strength of the interaction between two components. The weighted average is obtained when K=1. And when $K<1$, the T_g is lower than the weighted average, which suggests weak interaction. On the other hand, when $K>1$, the T_g is higher than the weighted average, which suggests strong interaction. For CPE32/DBS, the experimental value of T_g is in good agreement with the calculated value of T_g for $K=0.62$ as shown in Figure 7. This means the interaction between CPE32 and DBS is weak.

Secondly, in order to investigate the influence of the chlorine content of CPE on viscoelasticity and morphology, we carried out DMA and DSC measurements for CPE40/DBS. Figure 8 (a), (b) and (c) shows the temperature dependence of *E'*, *E"* and $\tan\delta_E$ of CPE40/DBS with different ϕ_{DBS}, respectively. As in the case of Figure 2, it was observed that T_g shifted to higher temperature and temperature width of the glass transition became narrow with ϕ_{DBS}. However, a small relaxation (β-relaxation) peak of *E"* in Figure 8 (b) was observed around -15 ^oC for CPE40/DBS, not observed for CPE32/DBS. This peak was observed for pure CPE40 and decreased with DBS content and then it disappeared for CPE40/DBS above ϕ_{DBS} of 40 wt%. Moreover, this peak appears at a lower temperature than the α-relaxation of pure CPE40. CPE has the

chemical structure of a polyethylene chain with substituted chlorine atoms randomly distributed and has not only chloromethylene unit (HCCl) but also dichloromethylene unit (CCl_2). The chloromethylene unit forms the intermolecular and intramolecular hydrogen bond between the chlorine atom and the α-hydrogen atom in CPE. In contrast, the dichloromethylene unit forms no hydrogen bond, resulting in segmental motion at lower temperature than chloromethylene unit. The generation of the dichloromethylene unit decreases the chloromethylene unit. Thus, the local segmental motion, observed as β-relaxation, is caused by the sequence of the methylene and the dichloromethylene unit at lower temperature than T_g of CPE/DBS. In other words, the appearance of β-relaxation peak means an increase in dichloromethylene unit due to increase in chlorine content.

Figure 9 (a) and (b) show the dependence of E''_{max} and $\tan\delta_{Emax}$ on ϕ_{DBS} of CPE40/DBS, respectively. The values for CPE32/DBS are also shown as reference. E''_{max} of CPE40/DBS, as in the case of CPE32/DBS, increased in proportion to ϕ_{DBS} and increased rapidly above ϕ_c. The value of ϕ_c for CPE40/DBS is 23wt%. In comparison with CPE32/DBS, the value of ϕ_c shifted to the lower DBS content. This is due to the decrease in the α-hydrogen atom in CPE by the generation of dichloromethylene unit. Furthermore, the decrease in the α-hydrogen atom leads to the presence of a higher number of free DBS molecules in CPE40/DBS than CPE32/DBS at

the same DBS content above ϕ_c. As a result, E''_{max} of CPE40/DBS was higher than that of CPE32/DBS. On the other hand, E''_{max} of CPE40/DBS was lower than that of CPE32/DBS below ϕ_c, because of the separation of α- and β-relaxation and the decrease in the interaction between the α-hydrogen atom and the chlorine atom and between the α-hydrogen atom and DBS molecule by the decrease in the α-hydrogen atom. The value of $tan\delta_{Emax}$ of CPE40/DBS also showed a similar tendency with CPE32/DBS and is higher than that of CPE32/DBS in all DBS content.

Figure 10 shows DSC curves for CPE40/DBS. Crystallization peak was observed around 80 ^{o}C and melting peak around 100 ^{o}C for the CPE40/DBS with higher DBS content than 60 wt%. Table 2 shows the temperature and enthalpy of crystallization (T_c and ΔH_c) and melting (T_m and ΔH_m) peaks of CPE32/DBS and CPE40/DBS with the higher DBS content than 60 wt%. As in the case of CPE32/DBS, it was found that quenched CPE40/DBS also formed amorphous phase. The amount of DBS crystals forming during the heating process increases with ϕ_{DBS}, resulting from an increase in free DBS. However, in spite of CPE40/DBS having more free DBS than CPE32/DBS at the same DBS content, there is much less amount of DBS crystal in CPE40/DBS. In comparison with DBS molecules in CPE32/DBS, those in CPE40/DBS have lower molecular mobility and hence aggregate to crystallize with more difficulty, because of higher T_g.

Figure 11 shows the dependence of the middle point (T_g), the onset and the endset temperature of glass transition obtained from Figure 10 on ϕ_{DBS}. The value of T_g increased with ϕ_{DBS}, and then its slope of T_g against ϕ_{DBS} became gentle above the DBS content of 40 wt%. Considering onset and endset temperatures in Figure 11, the difference between the two temperatures was highest for pure CPE and decreased with increasing ϕ_{DBS} below the DBS content of 40 wt% and then became constant or slightly decreased above that. Endset temperature increased continuously, whereas onset temperature showed similar tendencies as T_g. It was, therefore, considered that the rapid increase in T_g below the DBS content of 40 wt% is caused by the β-relaxation which appears at a lower temperature than α-relaxation as previously mentioned in Figure 8. Because the α- and the β-relaxation temperatures are too close to separate as individual relaxations, the two relaxations were observed as one relaxation for CPE40/DBS with lower DBS content than 40 wt% in DSC measurement. As a result, a decrease in the onset temperature by β-relaxation led to a decrease in the apparent T_g judging from the onset and endset temperatures. In other words, the change in the slope of T_g against ϕ_{DBS} is caused by the appearance of β-relaxation in the lower ϕ_{DBS}.

Consequently, we observed lower ϕ_c, an decrease in E'' below ϕ_c and an increase in E'' above ϕ_c for the sample with higher chlorine content. The results here are contrary to those expected from the increase in the α-hydrogen atom by the increase in

the chlorine content. This is because the increase in chlorine content resulted in more dichloromethylene units, which decreases the α-hydrogen atom and causes β-relaxation. It is, therefore, necessary to take the amount of dichloromethylene unit into consideration, when investigating the influence of chlorine content on the viscoelasticity and morphology for CPE/DBS.

4. Conclusion

The viscoelasticity, morphology and the influence of the chlorine content on the characteristics of organic hybrid materials comprising of CPE and DBS were studied.

Both CPE32/DBS and CPE40/DBS are compatible blends at all DBS contents, resulting from DSC measurement. The value of T_g of CPE32/DBS increased with ϕ_{DBS} continuously and followed the Gordon-Taylor equation. On the other hand, the value of T_g of CPE40/DBS increased with ϕ_{DBS} and then became almost constant or slightly increased in the higher DBS content range. This change in tendency is caused by the appearance of β-relaxation of CPE40.

E''_{max} increased in proportion to ϕ_{DBS}, and then the slope of E''_{max} against ϕ_{DBS} became steep above ϕ_c. Below ϕ_c, DBS molecules dispersed in the CPE matrix, where a benzothiazolyl functional group in DBS interacted with the α-hydrogen atom in CPE. E''_{max} increased with ϕ_{DBS} by this interaction. A non-interacted α-hydrogen atom decreases with increasing ϕ_{DBS}, and then becomes zero at ϕ_c. Above ϕ_c, E''_{max} increased rapidly, because of free DBS molecules show high mechanical loss due to friction.

Increase in the chlorine content brought about the decrease in ϕ_c, the decrease in E''_{max} below ϕ_c and the increase in E''_{max} above ϕ_c. These results are contrary to expectation and they were caused by the dichloromethylene unit, which decreases the

α-hydrogen atom and generates β-relaxation. It was therefore necessary to take into consideration not only the chlorine content but also the amount of the dichloromethylene unit in CPE, while investigating the influence of chlorine content.

Acknowledgement

This study has been partially supported by The 21st Century Center of Excellence (COE) program "*Creation of Molecular Diversity and Development of Functionalities*" by the Japanese Ministry of Education, Culture, Sports, Science and Technology (MEXT), and Grant-in-Aid for Scientific Research (A) (16206066) from Japan Society for the Promotion of Science. Also, the support by the Eno Scientific Foundation is greatly acknowledged.

Reference

1. E. Hornbogen, in “Friction and Wear of Polymer Composites”, K. Friedrich, Ed., Elsevier Science, Amsterdam (1986) pp. 61-88.

2. K. Inoue, T. Itou, I. Matsuzaki, H. Kaneko, M. Kuromoto, M. Sumita, *Sen-i Gakkaishi*, **56**, 443-448(2000).

3. C. Wu, T. Yamagishi, Y. Nakamoto, S. Ishida, K. Nitta, S. Kubota, *J. Polym. Sci.: Part B: Polym Phys.*, **38**, 1341-1347(2000).

4. C. Wu, T. Yamagishi, Y. Nakamoto, S. Ishida, K. Nitta, S. Kubota, *J. Polym. Sci:. Part B: Polym Phys.*, **38**, 2285-2295(2000).

5. K. Inoue, T. Itou, T. Miura, H. Kaneko, M. Kuromoto, M. Sumita, *Nippon Gomu Kyokaishi*, **74**, 35(2001).

6. C. Wu, *J. Appl. Polym. Sci.*, **80**, 2468-2473(2001).

7. H. Kaneko, K. Inoue, Y. Tominaga, S. Asai, M. Sumita, *Mater. Lett.*, **52**, 96-99(2002).

8. D. I. Livingston and J. E. Brown, Jr., “Proceedings of the fifth International Congress on Rheology,” vol. 4, S. Onogi, Ed., Univ. Tokyo Press, Tokyo (1970) pp. 25.

9. D. J. Walsh, J. S. Higgins and Z. Chai, *Polymer*, **23**, 336-339 (1982).

10. Z. Chai, R. Sun, D. J. Walsh and J. S. Higgins, *Polymer*, **24**, 263-270(1983).

11. H. Ueda and F. E. Karasz, *Polym. J.*, **26**, 771-778(1994).

12. M. M. Coleman, E. J. Moskala, P.C. Painter, D. J. Walsh and S. Rostami, *Polymer*, **24**,1410-1414(1983).

13. G. Defieuw, G. Groeninckx and H. Reynaers, *Polymer*, **30**, 595-603(1989).

14. M. Gordon and J. S. Taylor, *J. Appl. Chem.*, **2**, 493-500(1952).

Figure 1

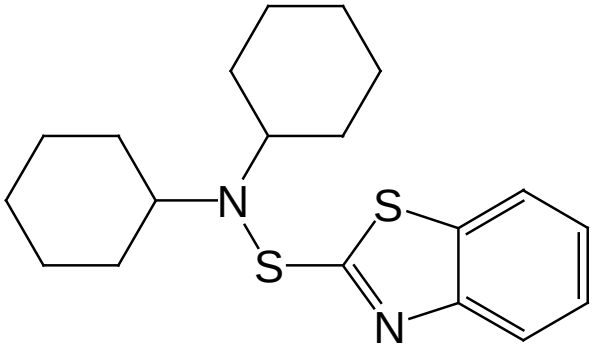

Figure 2

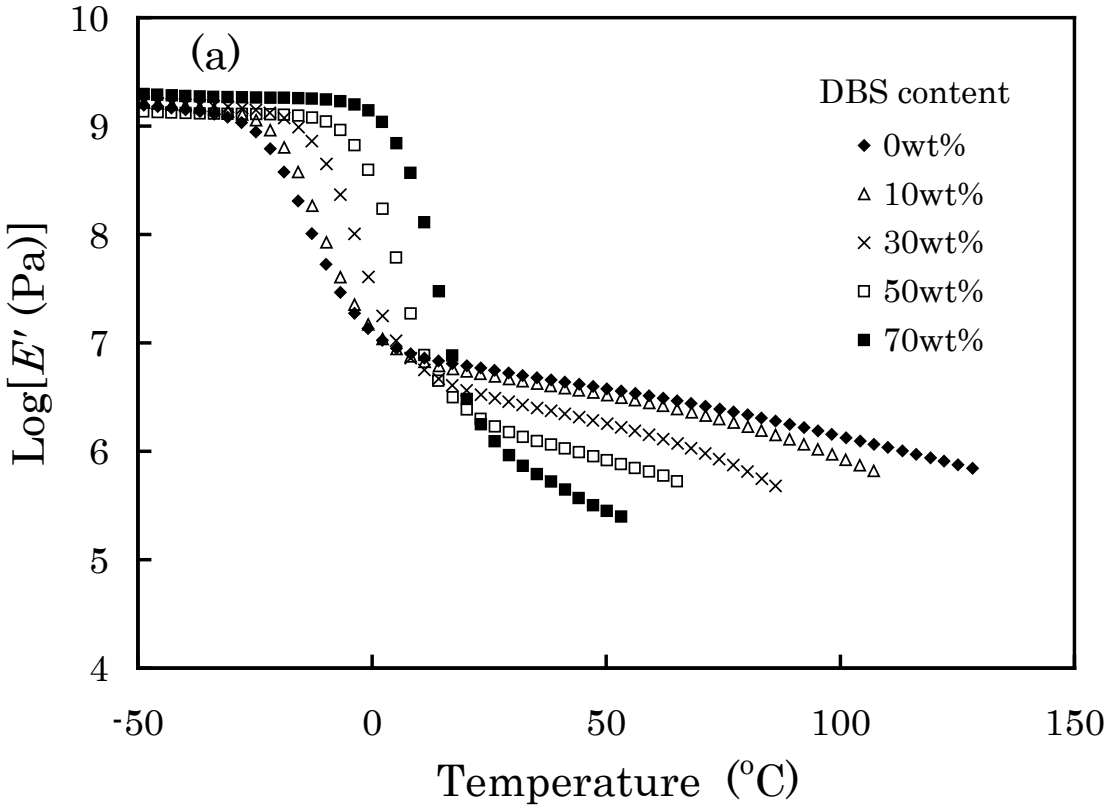
(a)
DBS content
0wt%
10wt%
30wt%
50wt%
70wt%
Log[E′ (Pa)]
10
9
8
7
6
5
4
-50
0
50
100
150
Temperature (°C)

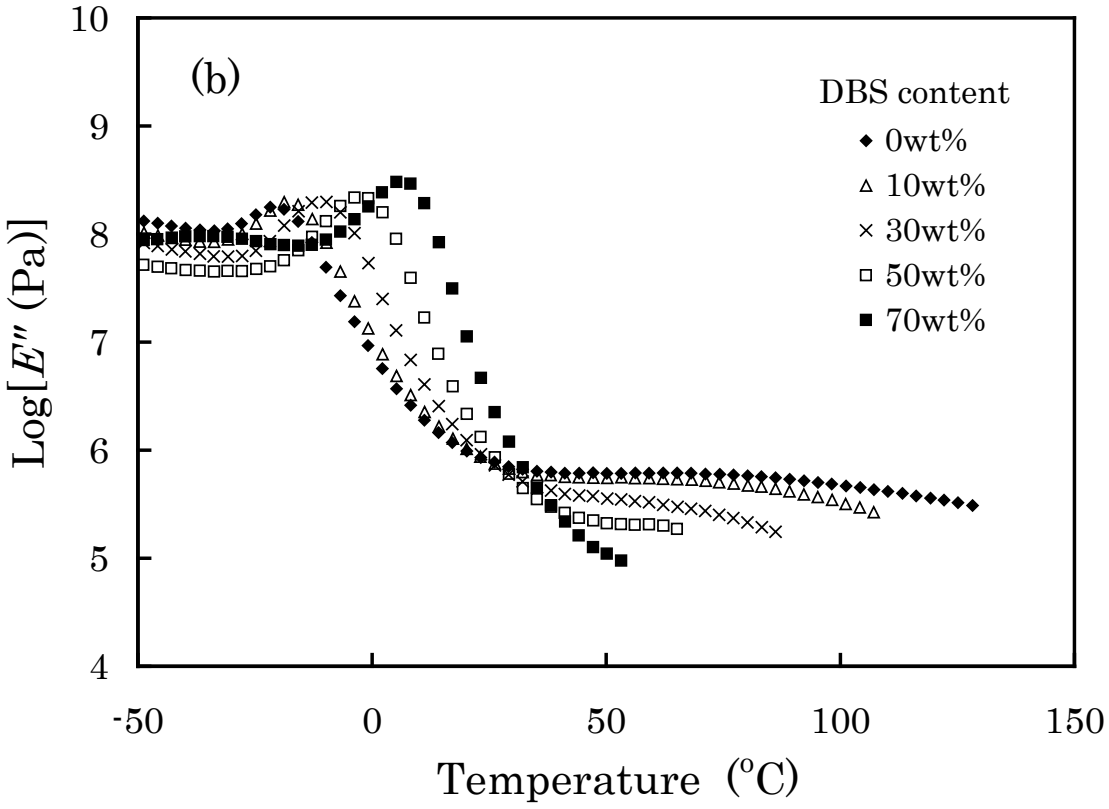
(b)
DBS content
0wt%
10wt%
30wt%
50wt%
70wt%
Log[E″ (Pa)]
10
9
8
7
6
5
4
-50
0
50
100
150
Temperature (°C)

Figure 2

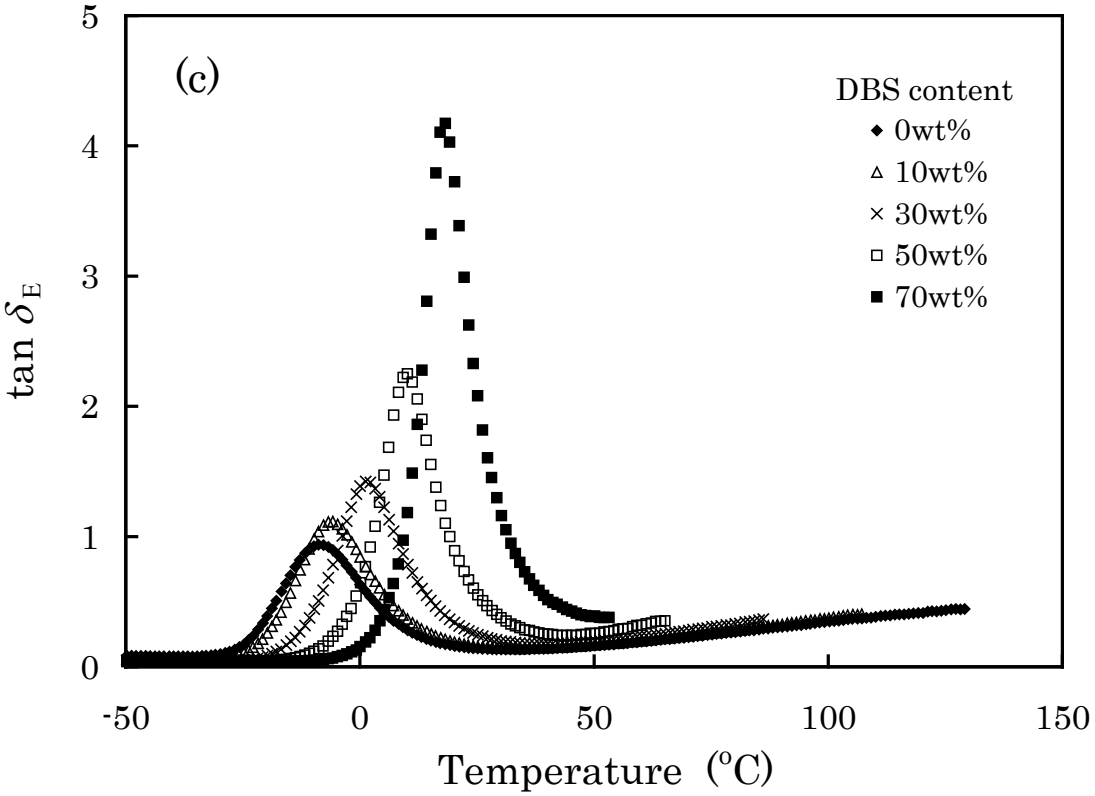
(c)
DBS content
0wt%
10wt%
30wt%
50wt%
70wt%
tan δ_E
0
1
2
3
4
5
-50
0
50
100
150
Temperature (°C)

Figure 3

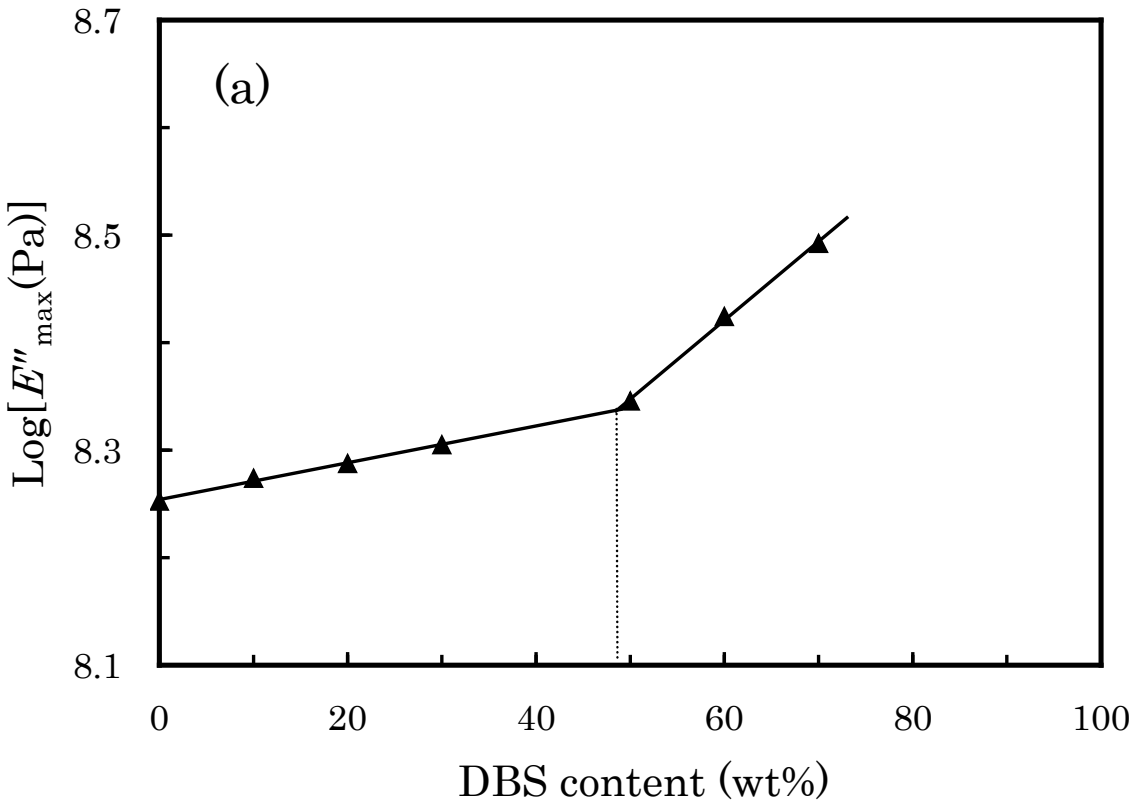
(a)
8.7
8.5
8.3
8.1
Log[E″max(Pa)]
0
20
40
60
80
100
DBS content (wt%)

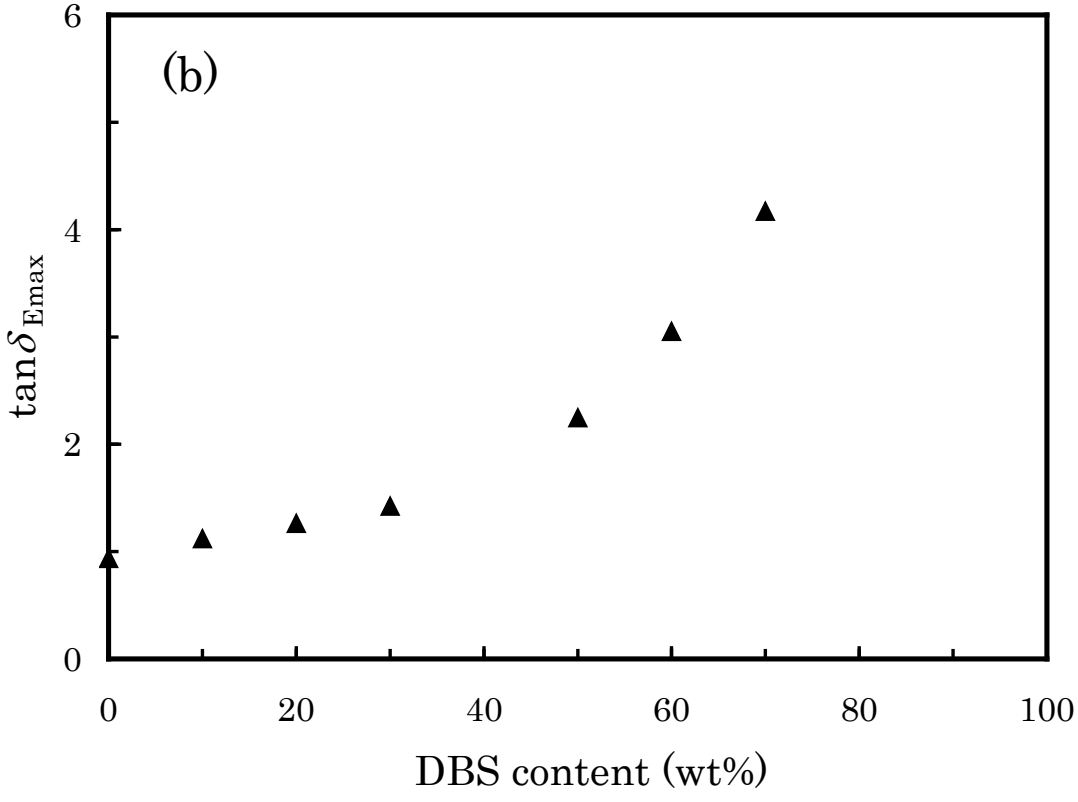
(b)
6
4
2
0
tanδEmax
0
20
40
60
80
100
DBS content (wt%)

Figure 4

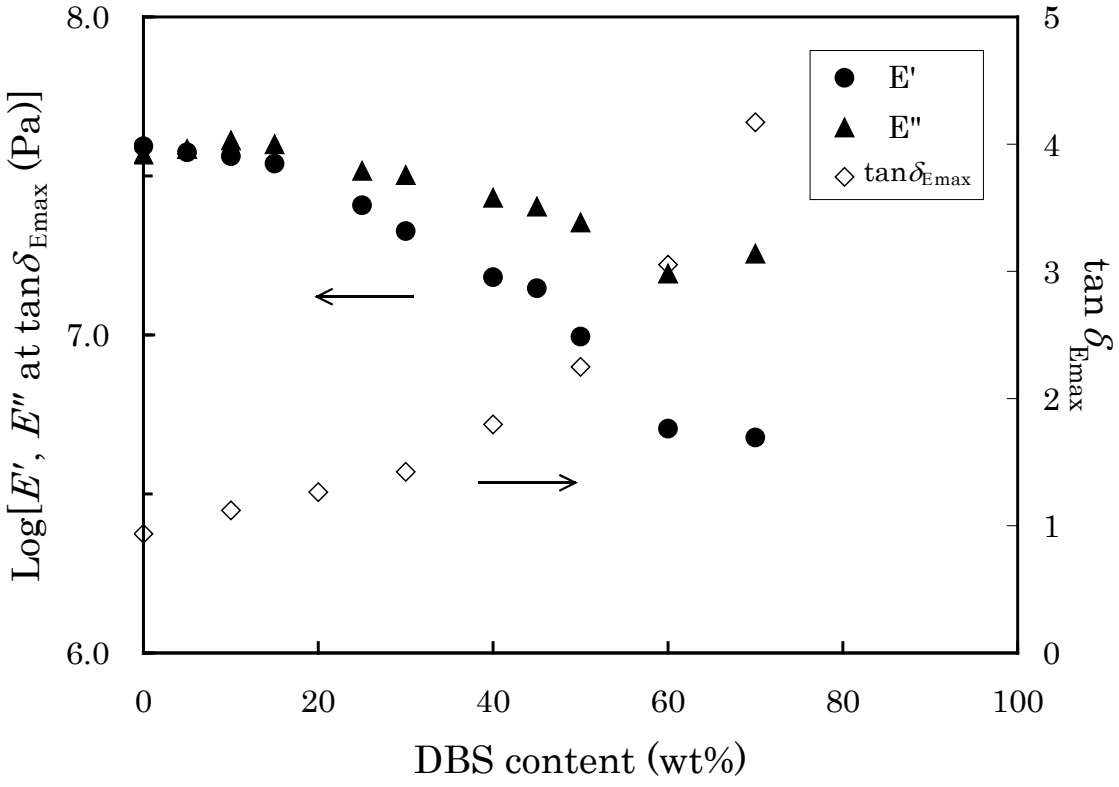
8.0
7.0
6.0
5
4
3
2
1
0
0
20
40
60
80
100
E'
E"
tanδEmax
Log[E', E" at tanδEmax (Pa)]
tan δEmax
DBS content (wt%)

Figure 5

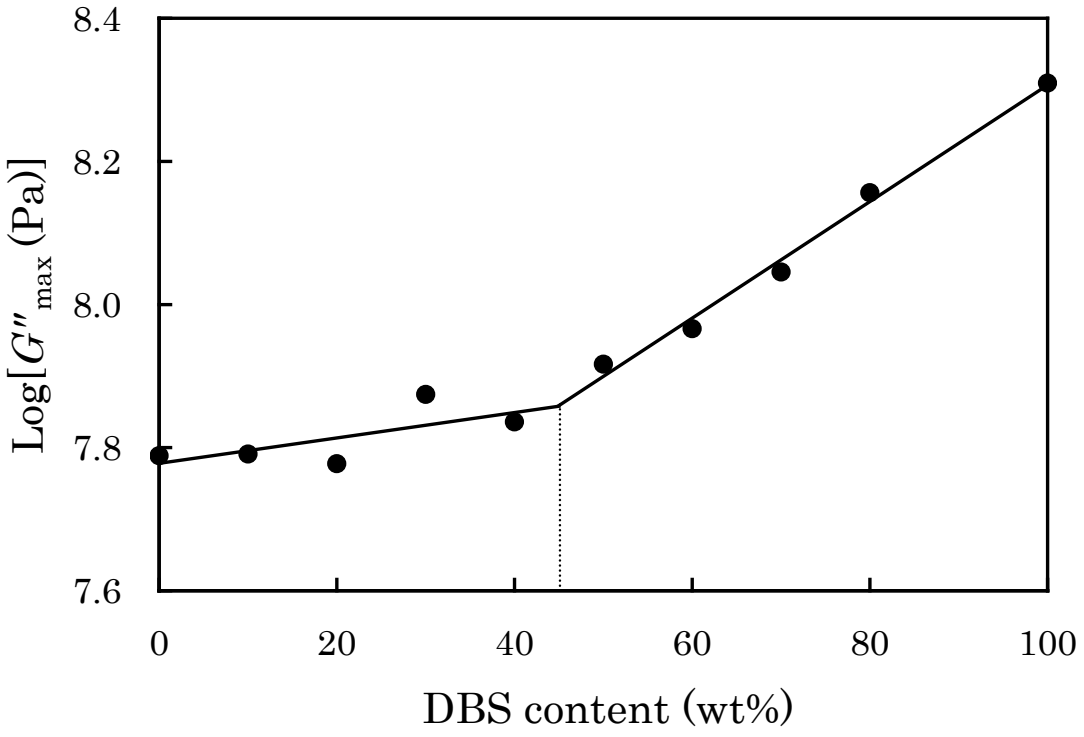

Figure 6

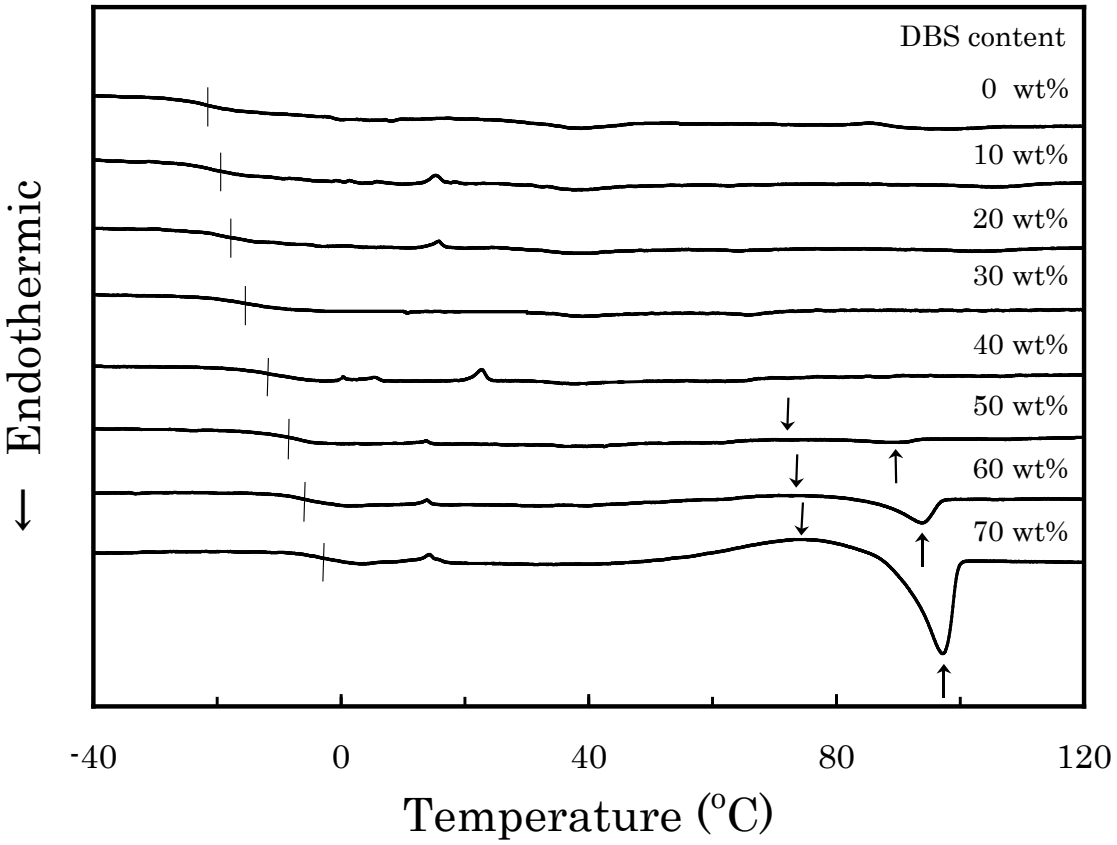
DBS content
0 wt%
10 wt%
20 wt%
30 wt%
40 wt%
50 wt%
60 wt%
70 wt%
↓ Endothermic
-40
0
40
80
120
Temperature (°C)

Figure 7

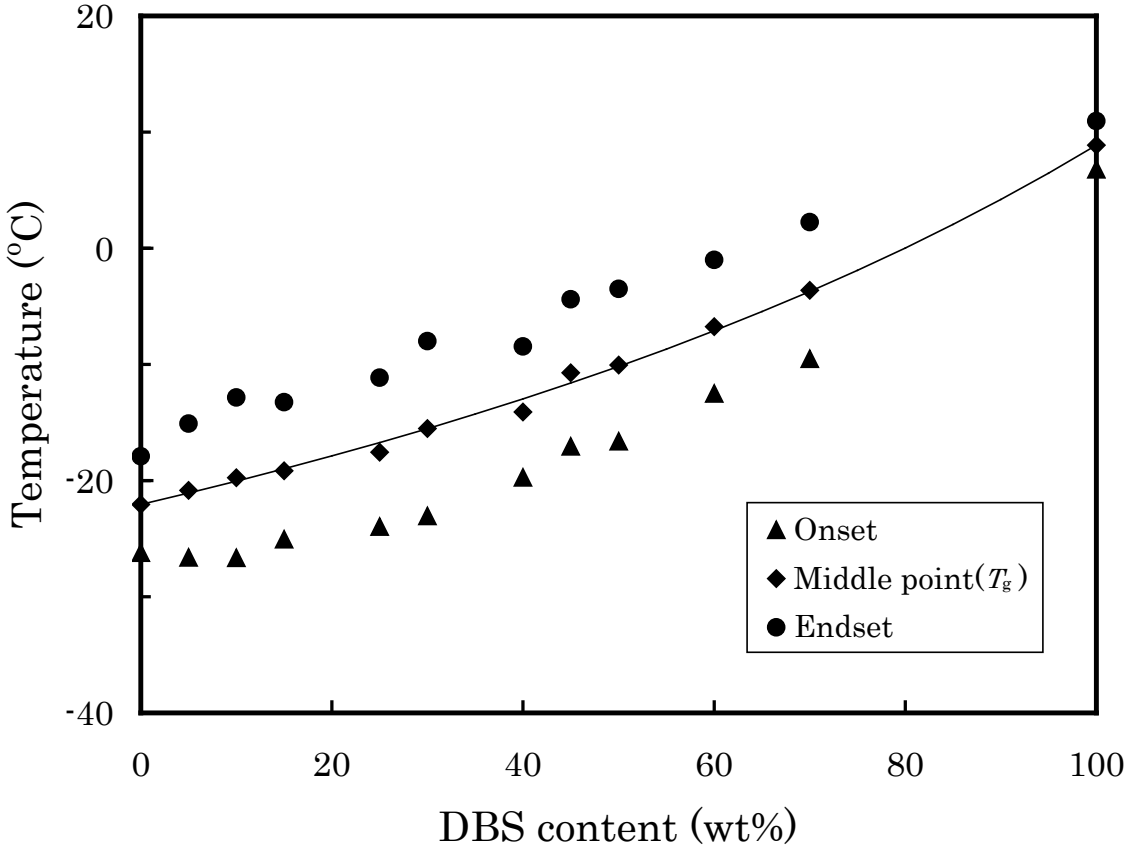
20
0
-20
-40
Temperature (°C)
0
20
40
60
80
100
DBS content (wt%)
Onset
Middle point(T_g)
Endset

Figure 8

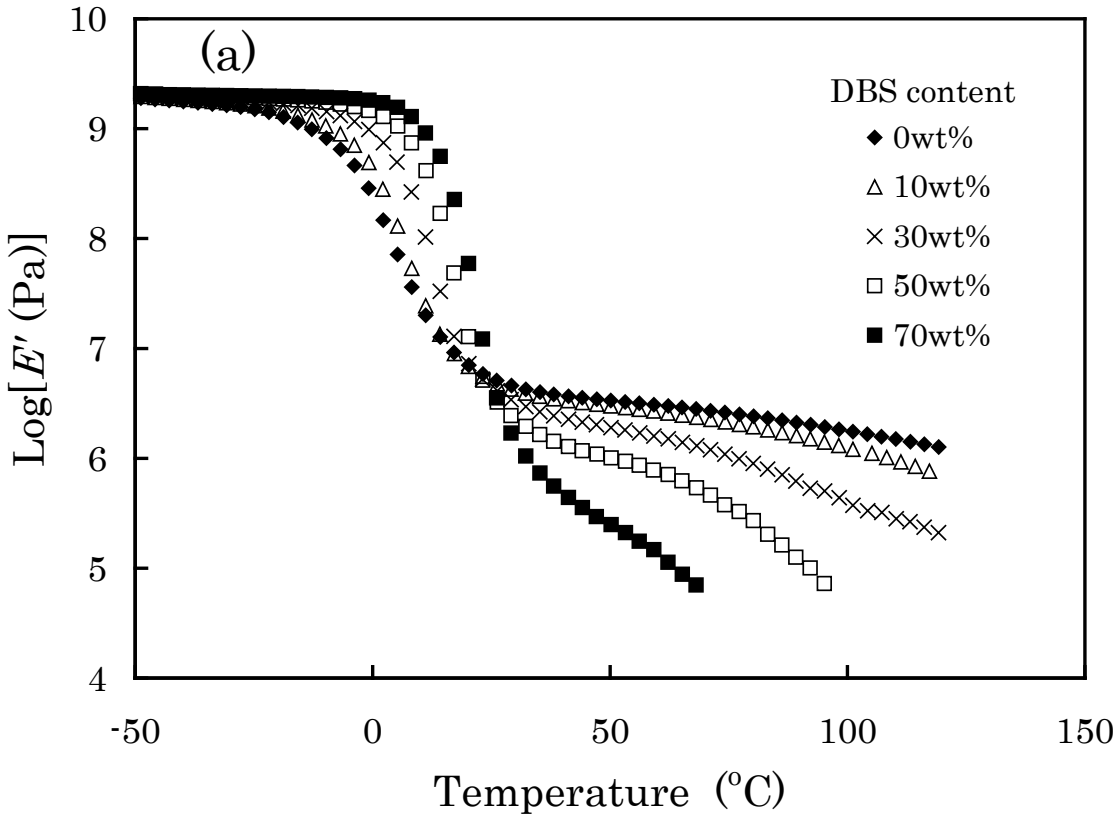
(a)
DBS content
0wt%
10wt%
30wt%
50wt%
70wt%
Log[E′ (Pa)]
Temperature (°C)
10
9
8
7
6
5
4
-50
0
50
100
150

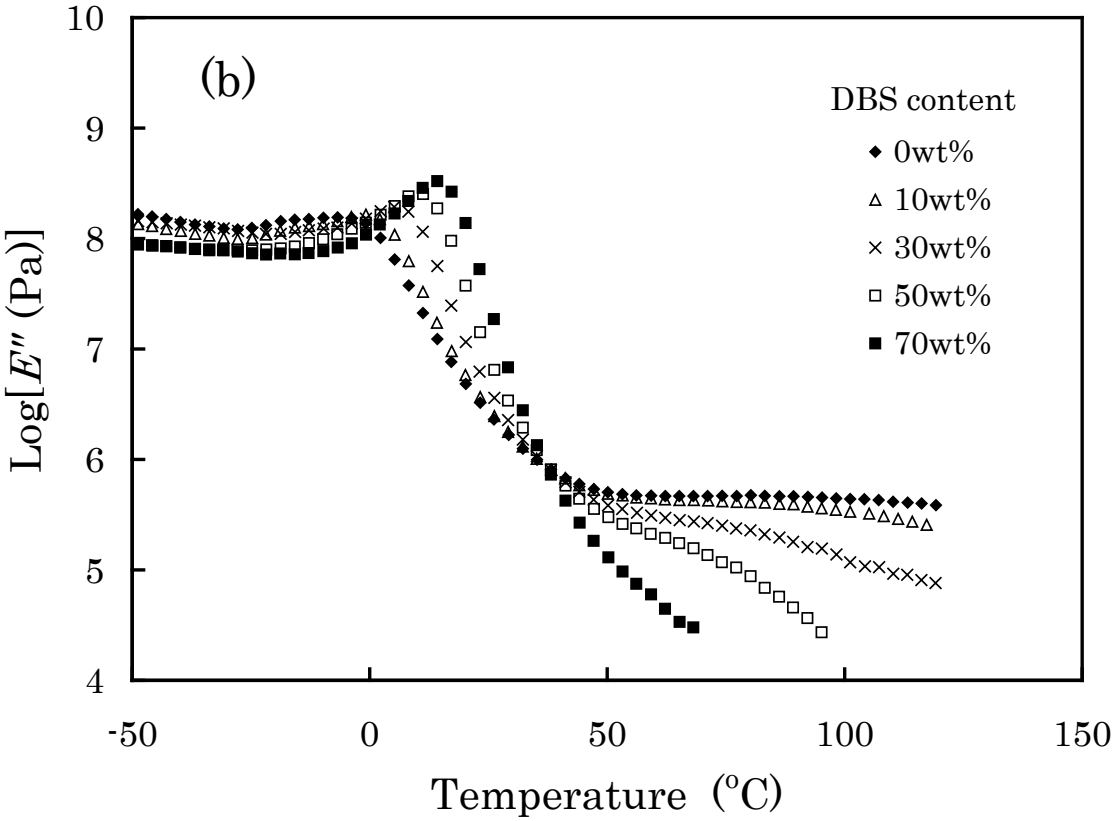
(b)
DBS content
0wt%
10wt%
30wt%
50wt%
70wt%
Log[E″ (Pa)]
Temperature (°C)
10
9
8
7
6
5
4
-50
0
50
100
150

Figure 8

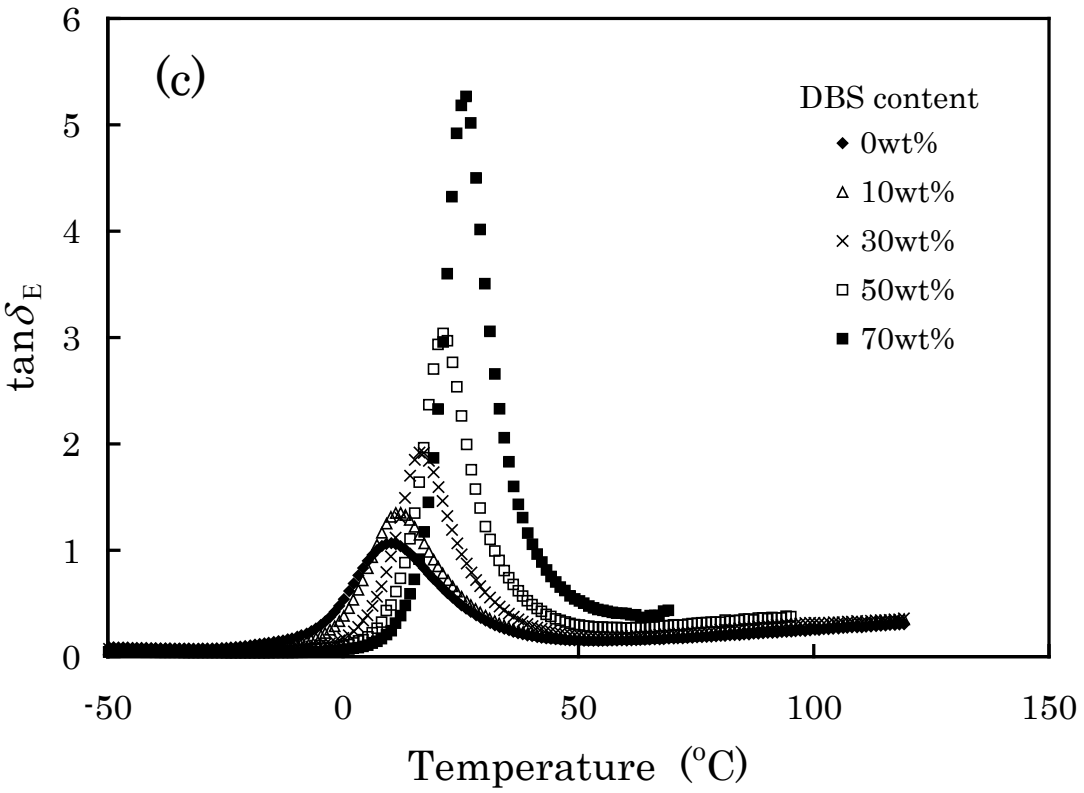
(c)
DBS content
0wt%
10wt%
30wt%
50wt%
70wt%
tanδE
6
5
4
3
2
1
0
-50
0
50
100
150
Temperature (°C)

Figure 9

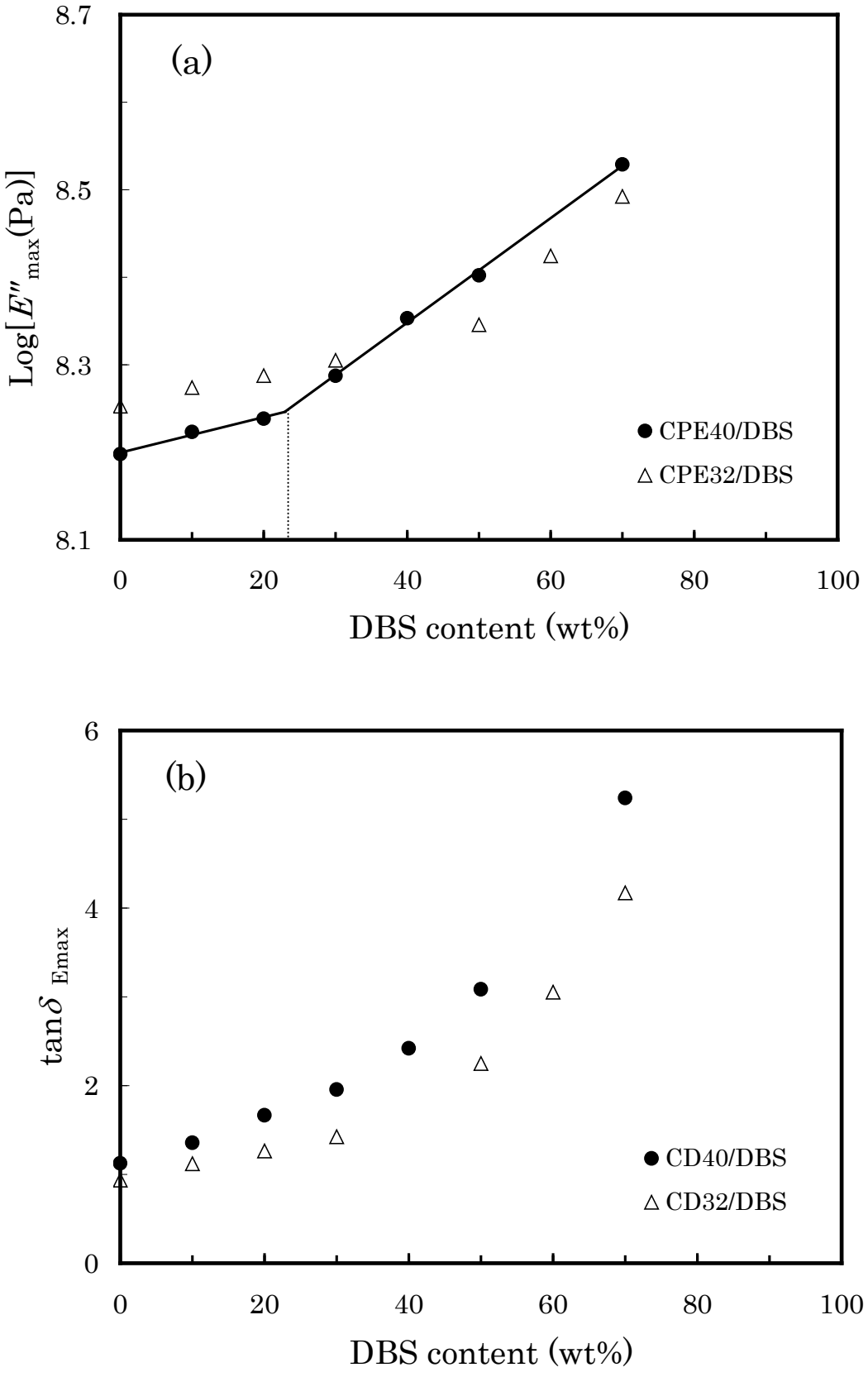
(a)
8.7
8.5
8.3
8.1
Log[E''max(Pa)]
0
20
40
60
80
100
DBS content (wt%)
CPE40/DBS
CPE32/DBS
(b)
6
4
2
0
tanδ Emax
0
20
40
60
80
100
DBS content (wt%)
CD40/DBS
CD32/DBS

Figure 10

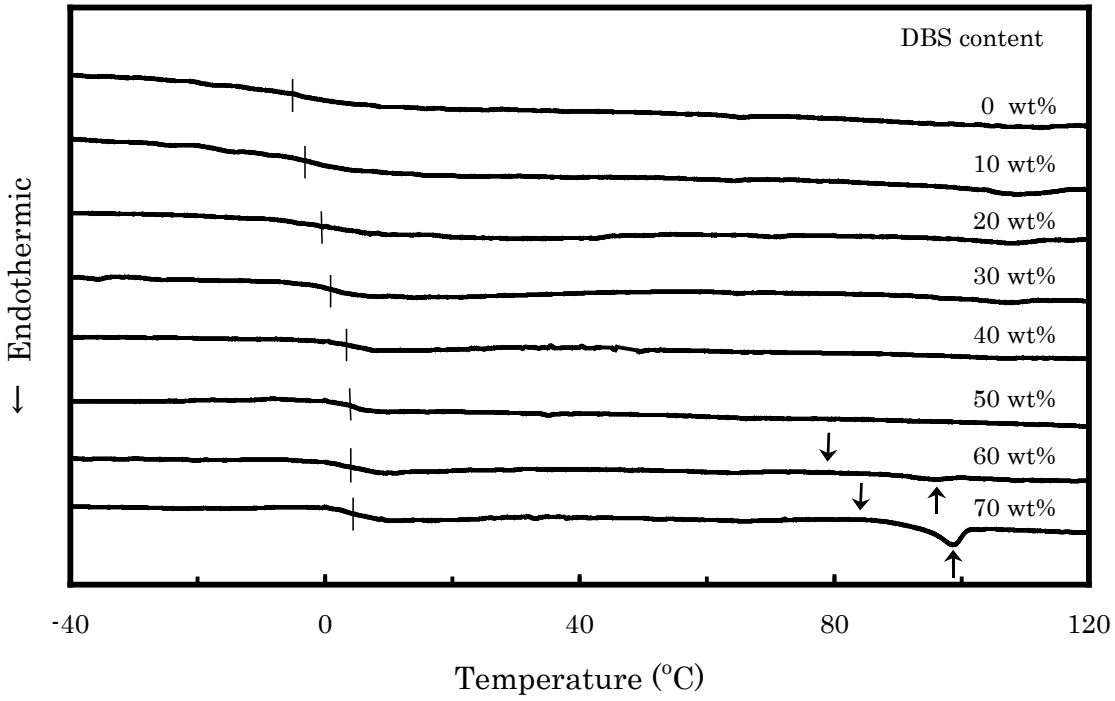
DBS content
0 wt%
10 wt%
20 wt%
30 wt%
40 wt%
50 wt%
60 wt%
70 wt%
← Endothermic
-40
0
40
80
120
Temperature (°C)

Figure 11

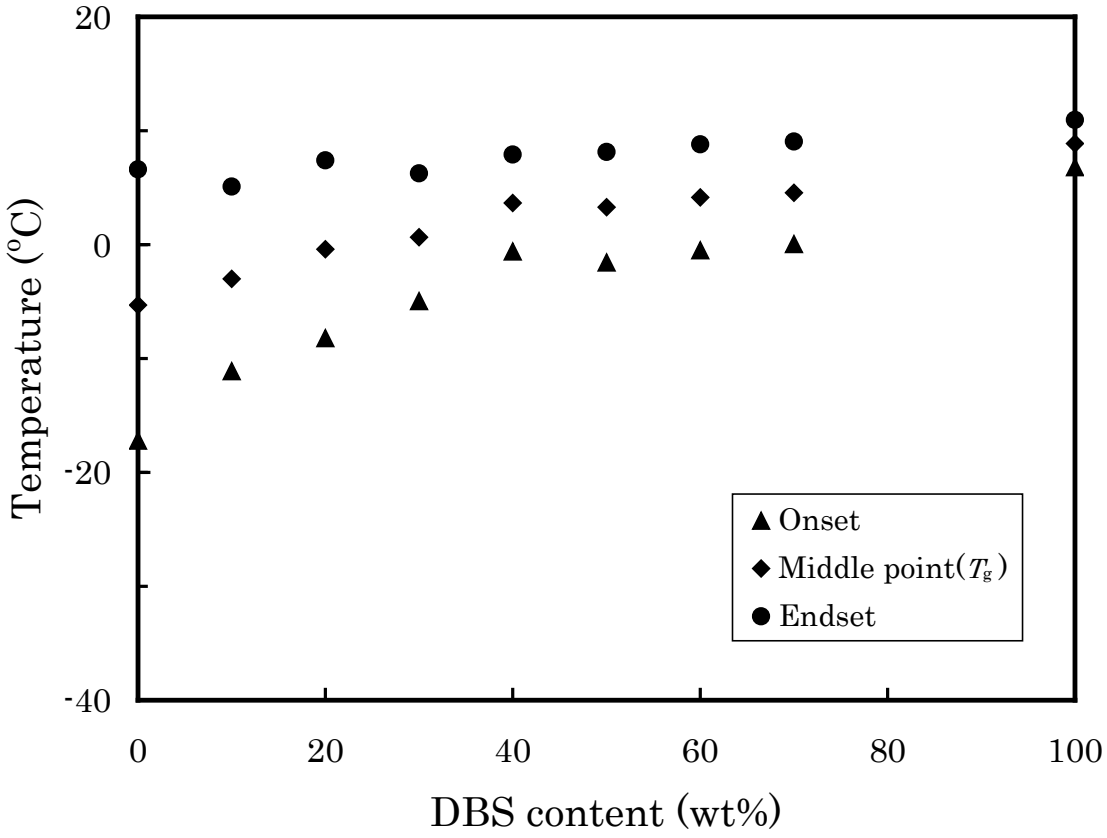
20
0
-20
-40
Temperature (°C)
0
20
40
60
80
100
DBS content (wt%)
Onset
Middle point(T_g)
Endset

Table 1

	Chlorine content	Molecular Weight		Polydispersity
	(wt%)	M_w ($\times 10^4$ g/mol)	M_n ($\times 10^4$ g/mol)	M_w / M_n
CPE32	32	31.3	7.79	4.02
CPE40	40	50.6	11.6	4.37

Table 2

	DBS content (wt%)	T_c (℃)	ΔH_c (J/g)	T_m (℃)	ΔH_m (J/g)
CPE32/DBS	60	71.9	3.04	93.7	3.22
	70	74.4	14.50	97.2	14.40
CPE40/DBS	60	79.2	0.73	95.8	0.35
	70	84.4	2.61	98.7	2.36
DBS	100	79.7	75.66	103.4	75.40

List of table and figure

Figure 8. Temperature dependence of tensile complex modulus of CPE40/DBS: (a) storage modulus, (b) loss modulus and (c) loss tangent.

Figure 9. Dependence of (a) E''_{max} and (b) $\tan\delta_{Emax}$ on DBS content of CPE40/DBS.

Figure 10. DSC curves of CPE40/DBS blends.

Figure 11. Dependence of onset, middle point (T_g) and endset temperature determined from Fig. 10 on DBS content of CPE40/DBS.

Table 1. Molecular weight of CPE measured by GPC

Table 2. Temperature and enthalpy of crystallization (T_c and ΔH_c) and melting (T_m and ΔH_m) peaks of CPE32/DBS, CPE40/DBS and pure DBS.